# Analyses of Injection and Falloff Data from DH4, Aug. 12 - Sept. 4, 2010

**Leif Larsen**
**Sept. 21, 2010**

# Table of Contents

# 1. SUMMARY

This report covers analyses of pressure transient injection and falloff data from the well DH4 carried out with the Saphir software from Kappa Engineering. The data set used in the analyses has been constructed from four separate tests run during the period August 12 - September 4, 2010, starting with a short minifrac test (Run 2) on August 12. The minifrac test was followed by a water injection and falloff test (Run 4) with 12 hours stable injection after an initial step-rate sequence and a little over 3.5 days shut-in period, another short minifrac test, and finally a long time test (LTT) with 5 days injection and 10 days shut-in starting August 19 and ending September 4. An overview of the tests is given in Table 1. Extended down-hole shut-in data will also be recorded in the well but not recovered in time for this report.

**Table 1 – Tests run in DH4.**

| | Injection | | | Falloff |
|---|---|---|---|---|
| | **fluid** | **hrs** | **m3/d** | **hrs** |
| **Run 2** | Viscous pill | 0.34 | 720 | 14.2 |
| **Run 4** | Water | 13.4 | 720 | 85.5 |
| **Run 5** | Viscous pill | 0.25 | 1332 | 18.6 |
| **LTT** | Water | 121.2 | 403.2 | 244.1 |

Prior to the start of injection an almost constant pressure of 29.6 bar (absolute) was recorded down-hole. With a gauge depth of 853 m below surface at the well site and 841 m below sea level, 82.4 bar would correspond to normal hydrostatic pressure at the gauge with the sea level as reference. This implies an under pressure of at least 52.8 bar in the formation if the recorded initial pressure is correct. From the falloff data it is not possible to give a reliable independent estimate of the formation pressure due to uncertain impact of nearby flow barriers, but values above 50 bar are not realistic.

Due to poor formation properties, substantial fracturing was expected and is also quite evident from the characteristics of the down-hole pressure data. Fracturing would normally lead to a significant improvement in well performance, but for DH4 it appears that there are sealing or partially sealing flow barriers in the formation with an adverse effect on the well performance. This is the most likely explanation for the observed pressure response, but other causes cannot be ruled out. One problem is that the falloff data from the tests are clearly dominated by linear flow (parallel flow lines perpendicular to the fracture surface or parallel to flow barriers), and such data cannot be used to determine the permeability without direct knowledge of the fracture or flow area, and vice versa. Another problem with efforts to determine permeability or fracture dimensions from linear-flow data is that the product of porosity and total compressibility enters directly into the computations, and that there can be considerable uncertainty in this value. Without extensive flow barriers in the formation, if that is the proper interpretation of the pressure response, one should be able to observe radial flow behaviour in late shut-in data and hence get a direct estimate of the formation permeability, but for DH4 this is not the case even with quite long shut-in periods. For

completeness, a short theoretical introduction to inherent problems in analyses of linear-flow data has been included in the report.

Even if there is considerable uncertainty in analyses of falloff data from DH4, there is at least some indication from the LTT falloff that the flow capacity is likely to lie somewhere near 45 md·m. This value has therefore been used as a base case in analyses with the added assumption that the net thickness is 30 m and hence the average permeability 1.5 md. With these values we get a fracture half-length of 400 m and the other key results listed in Table 2 from the LTT falloff. Guidelines on how to modify results if the thickness is changed but the flow capacity kept unchanged are given in Section 6.

| **Table 2 – Key base case results from the LTT falloff.** | | |
|---|---|---|
| Flow capacity (indicated) | 45 | md·m |
| Formation thickness (assumed) | 30 | m |
| Permeability (derived) | 1.5 | md |
| Fracture half-length (infinite conductivity) | 400 | m |
| Nearest boundaries (partially sealing) | 6, 20, and 35 | m (parallel to fracture) |
| Model initial pressure | 45.48 | bar (at gauge) |
| Radius of investigation | 406 | m (at 244 hrs) |

Table 3 lists the observed (transient) injectivity index from each of the four tests based on the three assumed values 30, 40 and 50 bar of the formation pressure. These numbers are just transient estimates of the actual long-term boundary dominated performance based on recorded pressures and rates, and not theoretical values. Theoretical values cannot be determined without known reservoir volume and flow properties. Another problem with these numbers is the fact that the injection takes place under fracture-growth conditions, with both rate and time affecting the results. For instance, for the two longest injection periods the down-hole pressure stayed fairly constant compared to the total pressure change through most of the injection periods. With fixed fracture dimensions a significant increase in pressure change would have been observed during the same periods, with a corresponding drop in the estimated injectivity index with initial pressure as reference.

| **Table 3 – Test performance (injectivity) data.** | | | | | |
|---|---|---|---|---|---|
| | **Test data** | | **Injectivity ($m^3$/d/bar)** | | |
| | **Rate** | **pwf** | **Reference pressure (sensitivity)** | | |
| | **m3/d** | **bar** | **30** | **40** | **50** |
| **Run 2** | 720 | 124.7 | 7.60 | 8.50 | 9.64 |
| **Run 4** | 720 | 130.7 | 7.15 | 7.94 | 8.92 |
| **Run 5** | 1332 | 148.7 | 11.22 | 12.25 | 13.50 |
| **LTT** | 403.2 | 138.3 | 3.72 | 4.10 | 4.57 |

The adverse effect of partially sealing boundaries on the well performance can be estimated if we use the base-case model from the analyses below as reference and determine how much the model data are affected if the barriers are removed. This exercise indicates that the injectivity from the LTT data set would increase by 52, 60 and 72% with initial pressures 30,

40 and 50 bar as reference if the partially sealing boundaries are removed. Note also that if we use the base-case model parameters from the LTT analysis without internal boundaries and an ideal fracture (no damage), then we get a stabilized injectivity index of 3.39 $m^3$/d/bar for the well at the centre of a 3x3 km square, with this value increased to 4.59 $m^3$/d/bar for a 2x2 km square. Considering the importance of the fracture, note for the a 3x3 km square that we get the injectivity index 0.46 $m^3$/d/bar with just the small bore-hole and no fracture, and the values 1.15, 1.39, 1.73, 2.30, 2.84 and 3.39 $m^3$/d/bar for infinite-conductivity fractures with half-length 25, 50, 100, 200, 300 and 400 m.

The following points summarize key observations, challenges and results from the DH4 data:

- Formation is under-pressured
- Well clearly fractured
- Not possible to determine permeability directly
- Not possible to determine fracture dimension without known permeability
- Reduced lateral connectivity in the reservoir with sealing or partially sealing barriers parallel to the fracture
- The main results from the analyses are qualitative and suggest formation scenarios that can explain the pressure response observed through the test sequence

The points above are addressed in detail below.

# 2. BACKGROUND INFORMATION AND TEST DATA FROM DH4

## 2.1. Formation properties

Figure 1 shows a lithology log covering the bottom 300 m in DH4 from 670 m and down to 970 m, with the best zones indicated. In the base case of the analyses it has been assumed that injection takes place in the best 30 m of sand as net thickness with an assumed average permeability of 1.5 md. Additional alternative analyses have also been included in the report with the same flow capacity of 45 md·m and thickness increased to 90 m, and hence average permeability reduced to 0.5 md, and a case with the same permeability of 1.5 md but increased thickness to 100 m, and hence flow capacity increased to 150 md·m. The three cases have been included in the report to illustrate the non-uniqueness of the data.

Since injection takes place into the lower 100 m and the well is clearly fractured, there is considerable uncertainty about the vertical height of the fracture. It can stay in the best sands with limited height, as assumed in the base, it can cover the 100 m of open interval, or it can extend above the packer. For the analyses and also for the performance of the well, the actual height of the fracture is not important, what matters is the net sand thickness, i.e., the sum of the intervals with enough permeability to allow injection.

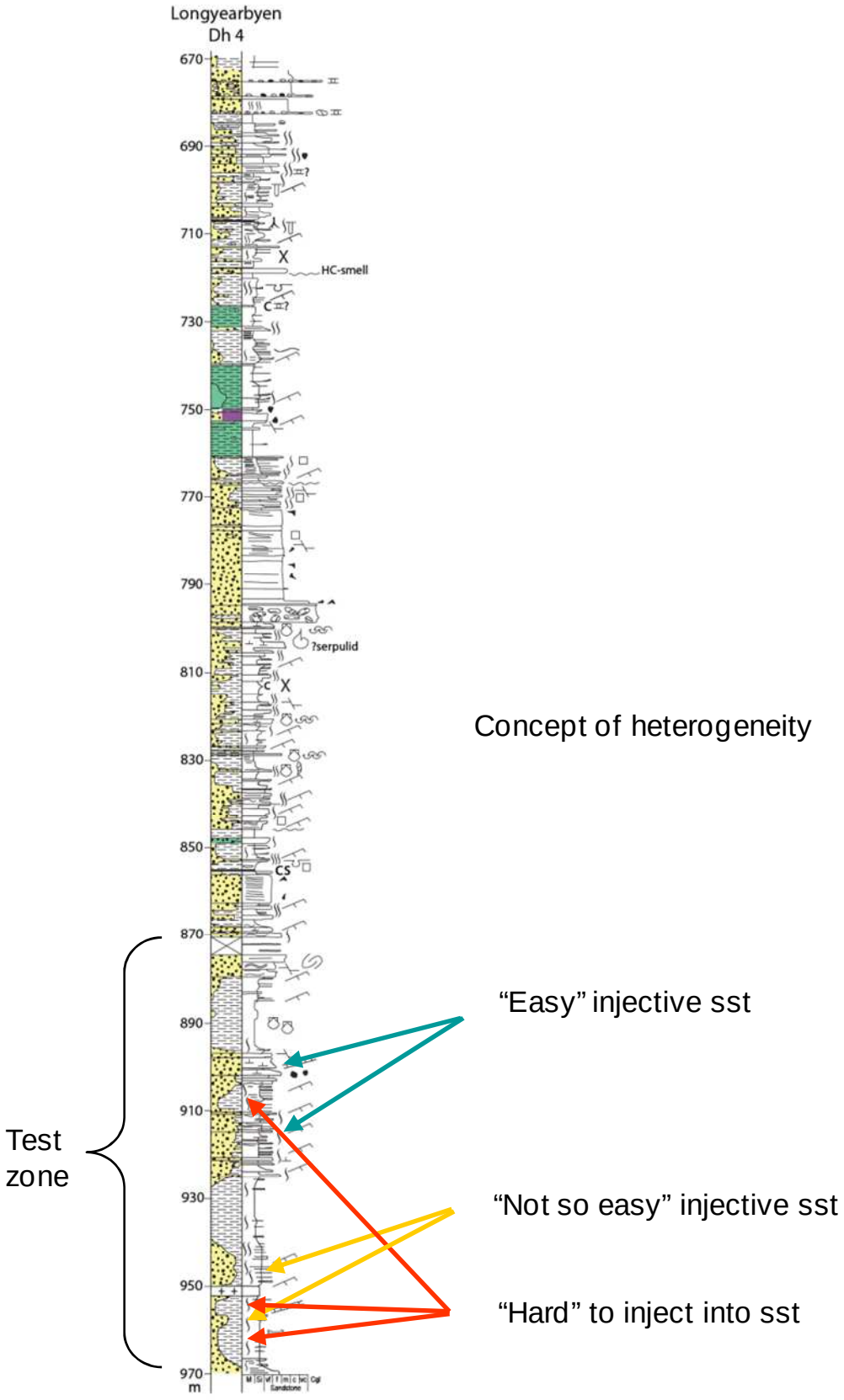


**Figure 1 – Concept of heterogeneity of the well DH4.**

Analyses of the dynamic data from DH4 also depend on static data such as thickness and PVT parameters. The values listed in Table 4 have been used in all analyses. Of these, the total compressibility is perhaps most uncertain.

| **Table 4 – Basic parameters used for all analyses.** | | |
|---|---|---|
| Volume factor | 1.0 | $Rm^3/Sm^3$ |
| Viscosity | 0.5 | cp |
| Porosity | 0.1 | |
| Total compressibility | 5E-5 | 1/bar |
| Wellbore radius | 0.023 | m |
| Gauge depth | 853 | m |

## 2.2. Rates and Down-Hole Data from DH4

Temperature and pressure data from the four tests in DH4 are shown in Figure 2 with labels at the top and colour-coded temperature data delineating the four runs. Pressure data from the four test runs can also be delineated from the fact that each run starts and ends with the gauge at surface at atmospheric pressure (1.013 bar).

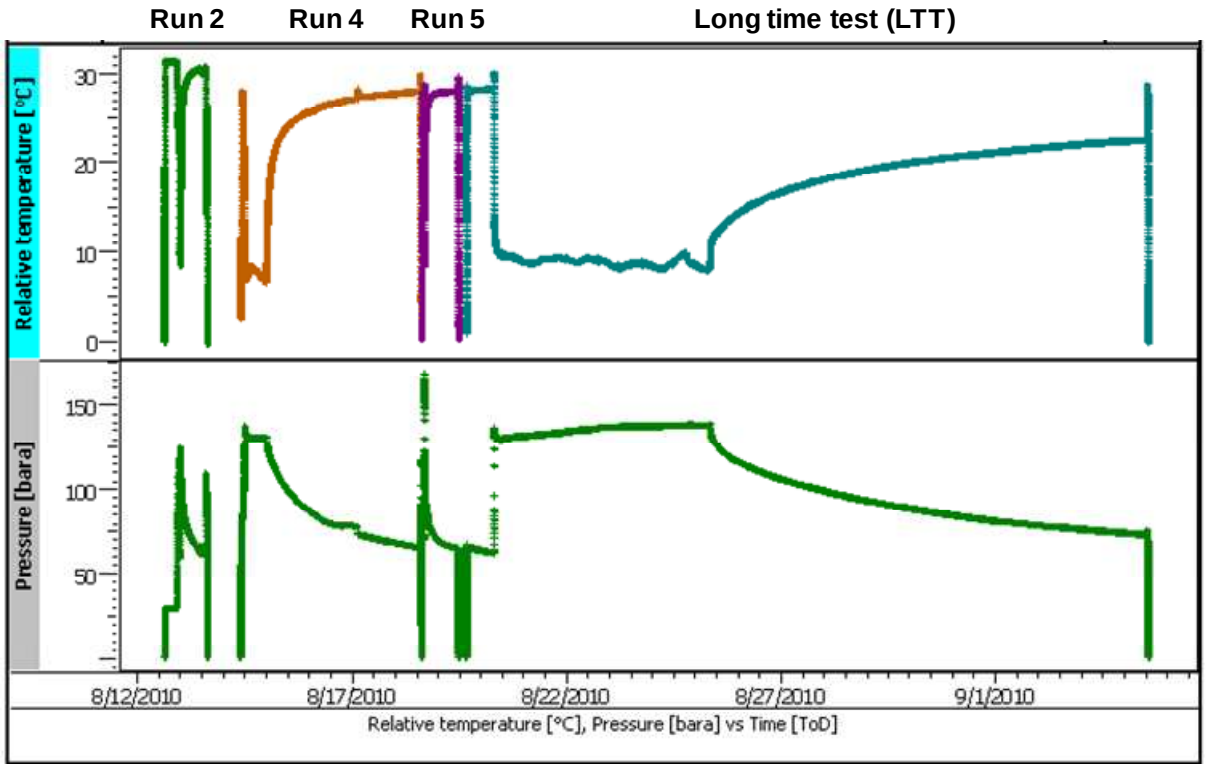


**Figure 2 – Temperature and pressure data from the complete test sequence.**

Figure 3 shows the pressure data and rate history used in analyses, with the four main falloffs identified. Only the falloffs can be used directly in analyses do to a non-static inner boundary of the flow caused by fracture growth and perhaps also changing skin from viscous pill injection for the minifrac tests.

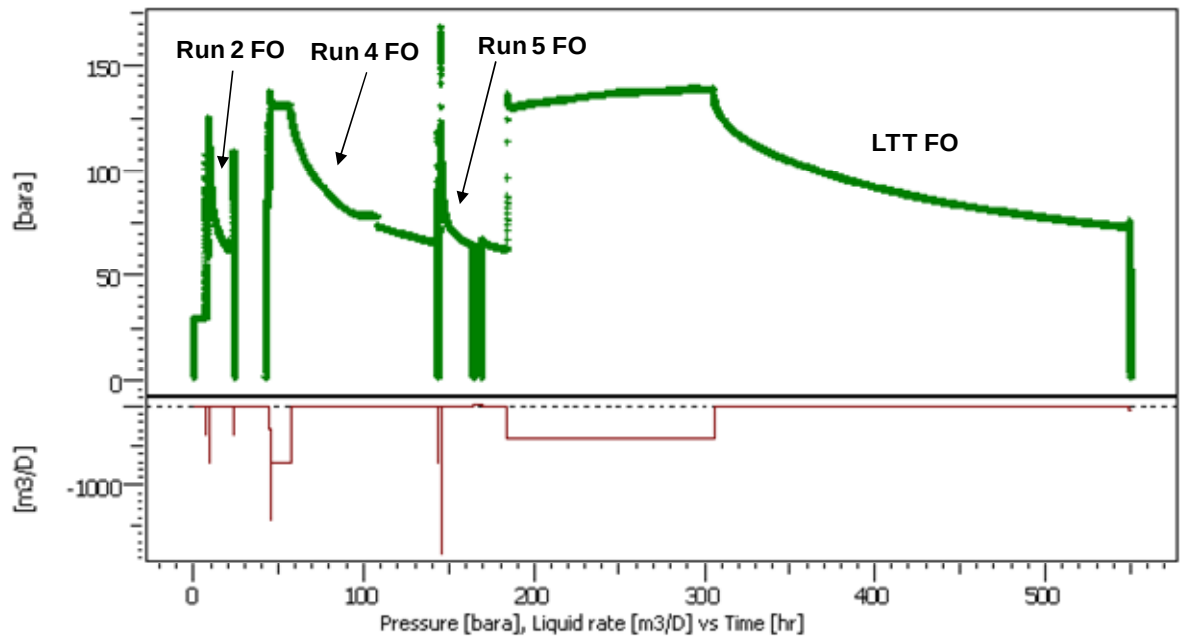


**Figure 3 – Merged pressure data and rate history used in analyses.**

Rather than observing a hydrostatic pressure of around 85 bar at the gauge depth, a clear under pressure was recorded prior to the injection. The pressure was not static but increasing slightly, with a value of 29.6 bar (absolute) recorded just before the injection started. This reference pressure has been indicated in Figure 4 as a dashed line. After the injection periods the pressure should decline towards this reference level, at least for the first falloff. However, except perhaps for the very first falloff, this does not appear to be the case. Actually, from Figure 4 the reservoir pressure appears to be increasing through the test sequence as if the injection takes place into a small volume. Even if the average pressure shows a clear increase near the well it does not necessarily imply that the well only communicates with a small volume. It does, however, imply that there is poor communication between the well and the reservoir, most likely due to sealing or partially sealing barriers parallel to the fracture.

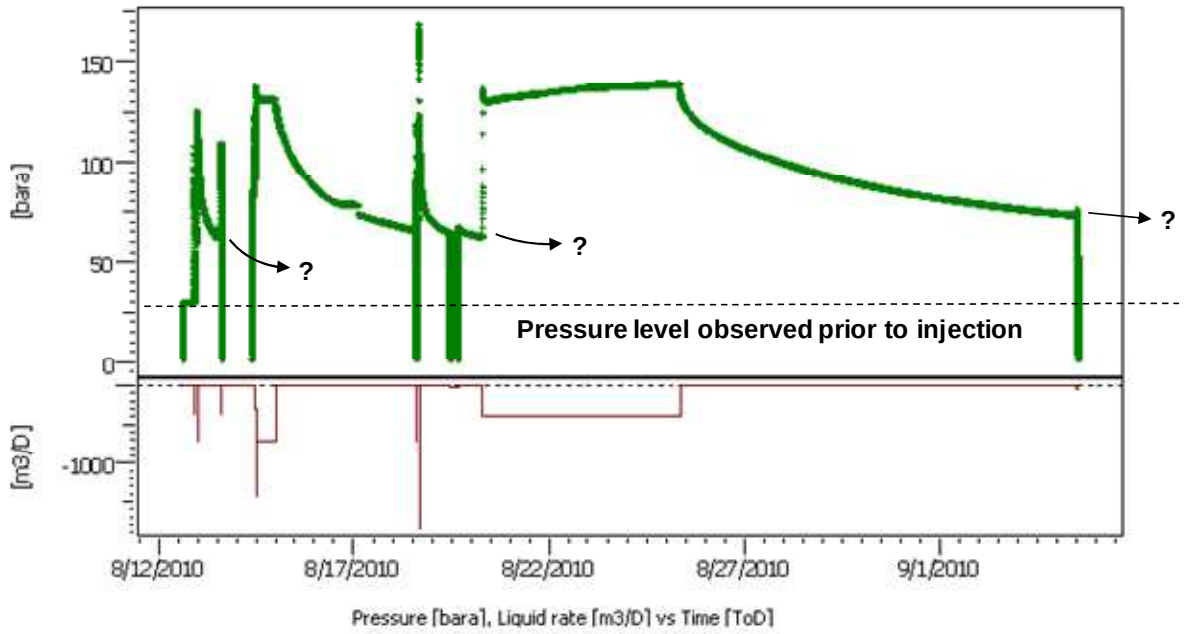


**Figure 4 – Observed down-hole pressure prior to injection compared to pressure decline trends after injection periods.**

In order to determine if the reservoir volume is indeed limited, or if only the pressure communication is limited, it is necessary to carry out detailed analyses of the data. Conclusions cannot be based on observation of an overview plot of the type shown in Figure 4 alone. The next section illustrates some of the key points.

## **2.3.** Characteristics of the DH4 Falloff Data

A combined loglog diagnostic plot of the main falloff from each of the four test runs in DH4 is shown in Figure 5. Each falloff is represented by two data sets: change in pressure since shut-in and logarithmic derivatives ("semilog slopes"), with the derivative data from the different tests identified in the relevant figures below. The derivatives are used both to identify flow regimes in analyses, such as radial, linear or spherical, and to determine model parameters from the value(s) of the derivatives. Since the diagnostic plots are normalized with respect to rate, the derivatives should overlap during the initial parts of the falloffs unless the flow pattern changes significantly near the well. From Figure 5 it is clear that we do not have a static well or fracture model throughout the test sequence, obviously caused by fracture growth during the longer injection periods. However, the early parts from the two minifrac tests (Runs 2 and 5) are quite similar. Early derivatives from the other two tests are also close, but they do not directly overlap. Part of the difference between early data from Run 4 and the LTT appears to be caused by poor data. This is pointed out below in the section covering analyses.

A special feature of the falloff data from the first three tests is that the derivatives start out below the corresponding pressure differences, as is normal, but cross over and end up above the pressure change data at the end of the falloff, which is quite unusual. This feature

is quite clear in Figure 6, which only includes the three first falloffs. The reason for this behaviour is a combination of fractures, nearby boundaries and short injection periods.

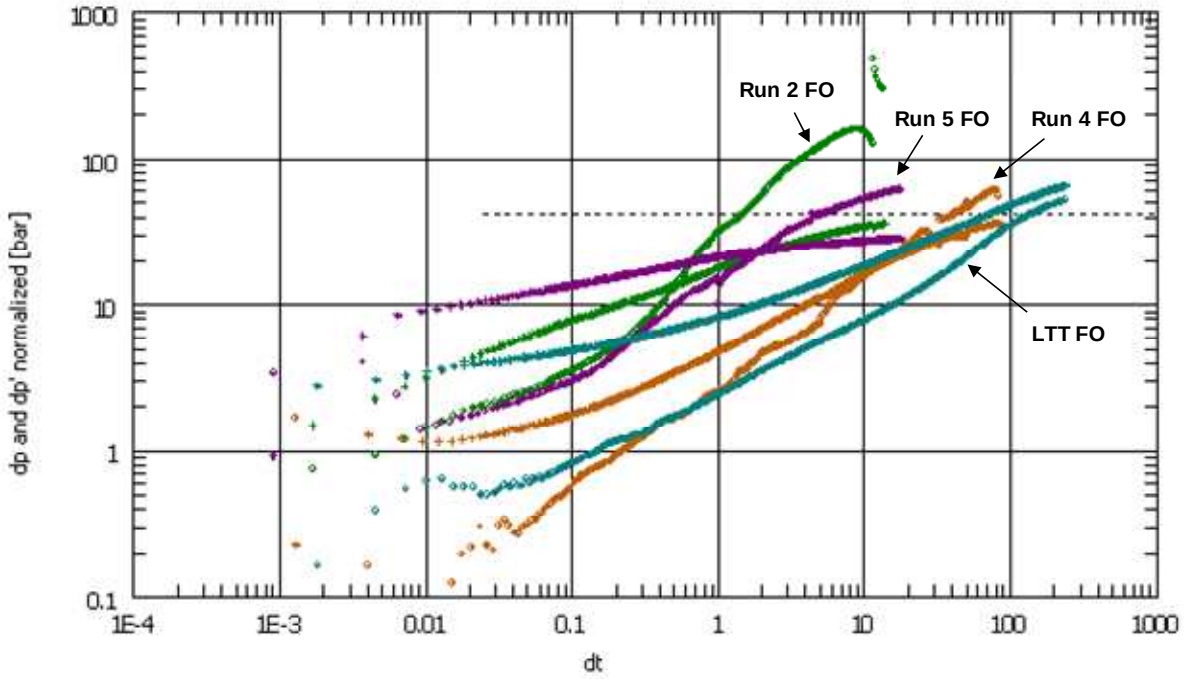


**Figure 5 – Loglog plot of the four key falloffs from DH4.**

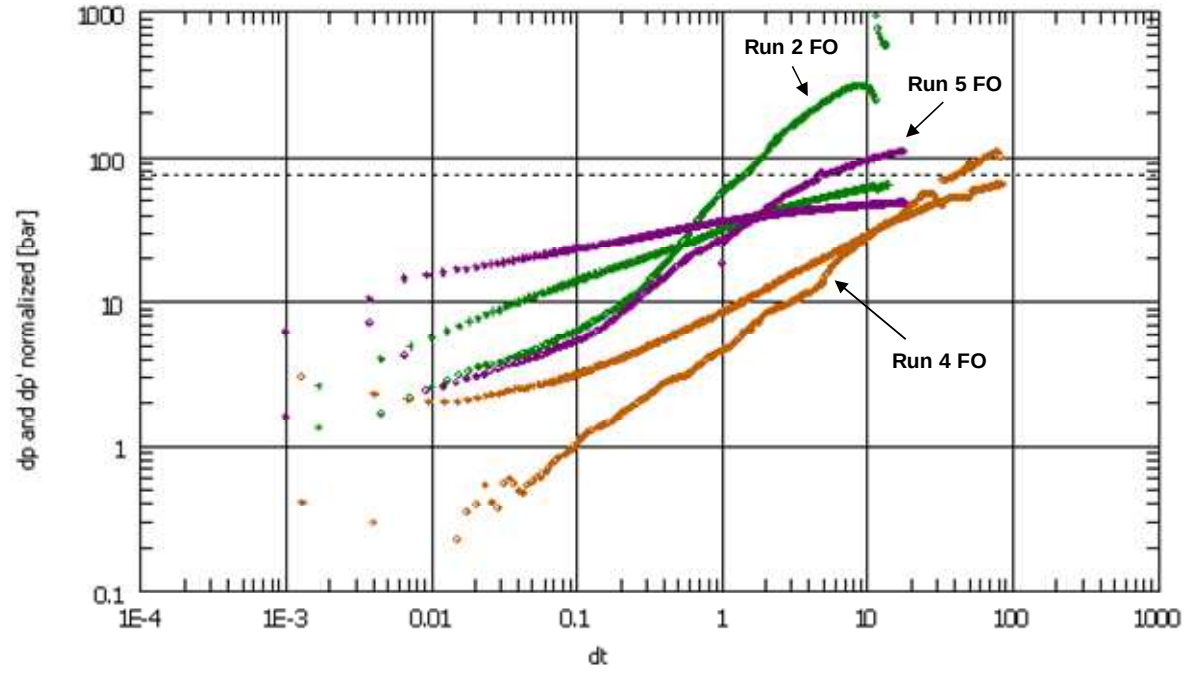


**Figure 6 – Loglog plot of the three first key falloffs from DH4.**

Figure 7 compares data from the two long falloffs. Although the derivatives from these falloffs are similar during a segment of early data, the overall behaviour of the two data sets are different. Actually, the LTT falloff data suggest that we have a simple fractured well near a no-flow boundary, while the falloff data from Run 4 does not exhibit a standard pressure response.

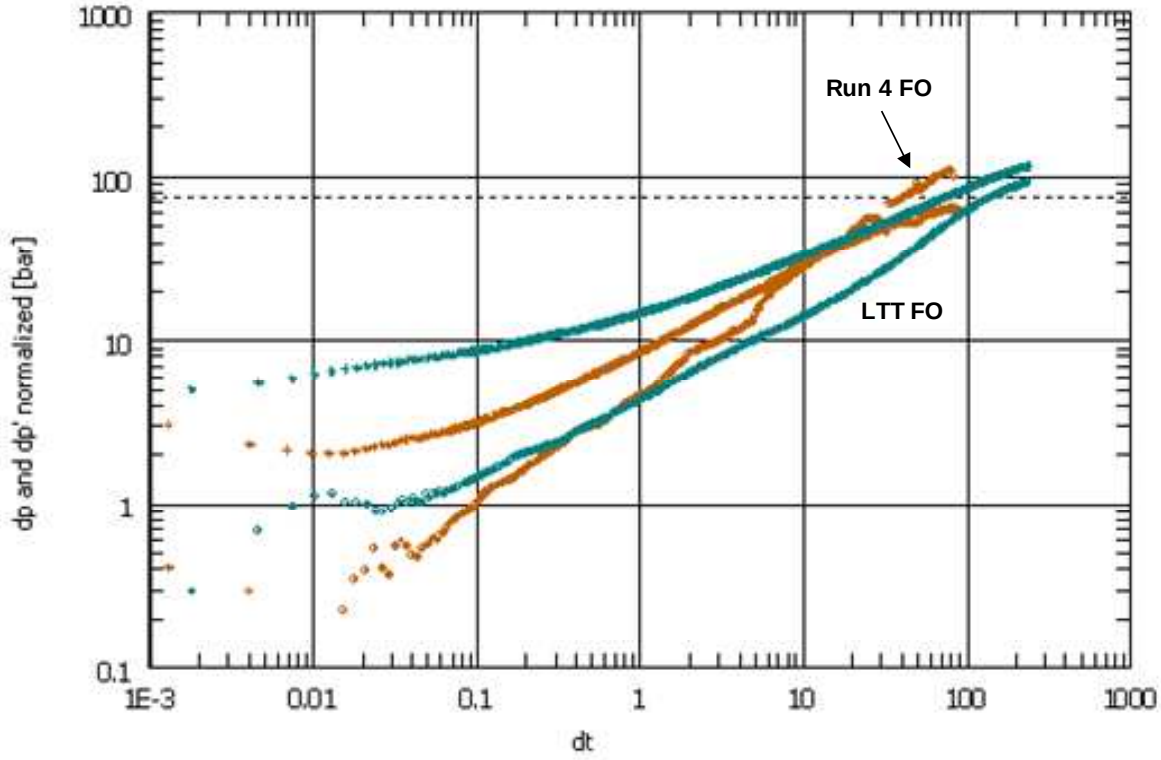


**Figure 7 – Loglog plot of the two longest falloffs from DH4 with significant injection prior to shut-in.**

Since the LTT falloff has a standard shape it can be used to illustrate key elements of data from fractured wells as shown in Figure 8. The upper data are the pressure changes since shut-in and the lower data the semilog slopes (derivatives with respect to natural logarithm of time, or actually of a special time expression).

The “half-slope” data in Figure 8 correspond to early data dominated by linear flow perpendicular to the fracture surface. Without any skin effect (no damage) the pressure changes and derivatives should be parallel with a separation of log(2) = 0.3. For the data set in Figure 8 it follows that a skin effect must be added to the fracture model.

For an unbounded model late derivative data should approach the dashed line in Figure 8. Since the derivatives after the half-slope period show an increasing trend with late data approaching a value at or close to twice the value of the dashed line, it is natural to assume that the fracture is located near a no-flow boundary. These assumptions, that we have a fractured well with damage and a nearby boundary, can be used as starting points for an analysis.

Since the other falloffs have very different characteristics it follows that even if a simple model can be found to match the LTT falloff, a more complex model will be needed to match all the falloffs. These ideas are pursued in the detailed analyses below.

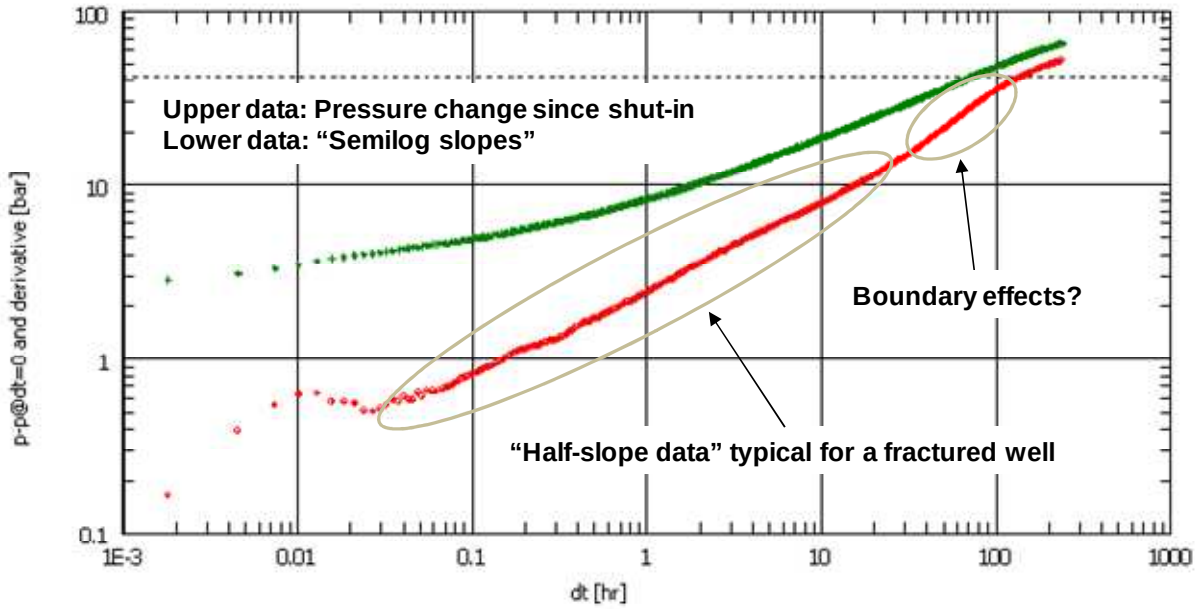


**Figure 8 – Loglog diagnostic plot of the falloff data from the long-time test.**

## 3. ANALYTICAL MODELS WITH FRACTURE AND A NO-FLOW BOUNDARY

### 3.1. Match of the LTT Falloff with Fracture and a No-Flow Boundary

Based on the characteristics of the data from the LTT falloff in Figure 8, a natural approach is to attempt to analyze the data with a vertical fracture and a nearby boundary. If that is a correct model, then the derivates should tend towards a level consistent with radial flow from one side (hemi-radial flow). This would roughly correspond to a flow capacity of 45 md·m with the given rate and basic parameters from Table 4 above. A base-case analysis has therefore been done with thickness 30 m and an average permeability of 1.5 md. This is in the expected range for the best sands indicated in Figure 1.

Figure 9 shows a match of the LTT falloff data with a uniform flux fracture with half-length 420 m and a parallel no-flow boundary at 50 m. Storage and damage have also been added in the model to improve the match of early data. Except for the segment of data between 1 and 10 hours after shut-in, the match is excellent. In the overview plot of the test data in Figure 10 the match of the falloff part of the LTT is also seen to be excellent, but the initial pressure of the model does not match the initial pressure measured in the well, nor does the model match the down-hole pressure during the 5 days of quite stable injection at 403.2 $m^3$/d (280 lpm). The failure to match the bulk of the injection data is normal with fracture propagation, as assumed, and the poor match of the initial pressure from the well is likely

caused by a discrepancy between the model and the complexity of the formation. Since the model has only a single boundary, it is not capable of reflecting a change in reservoir pressure during the test sequence, and will therefore decrease towards the initial pressure if the falloff is extended indefinitely.

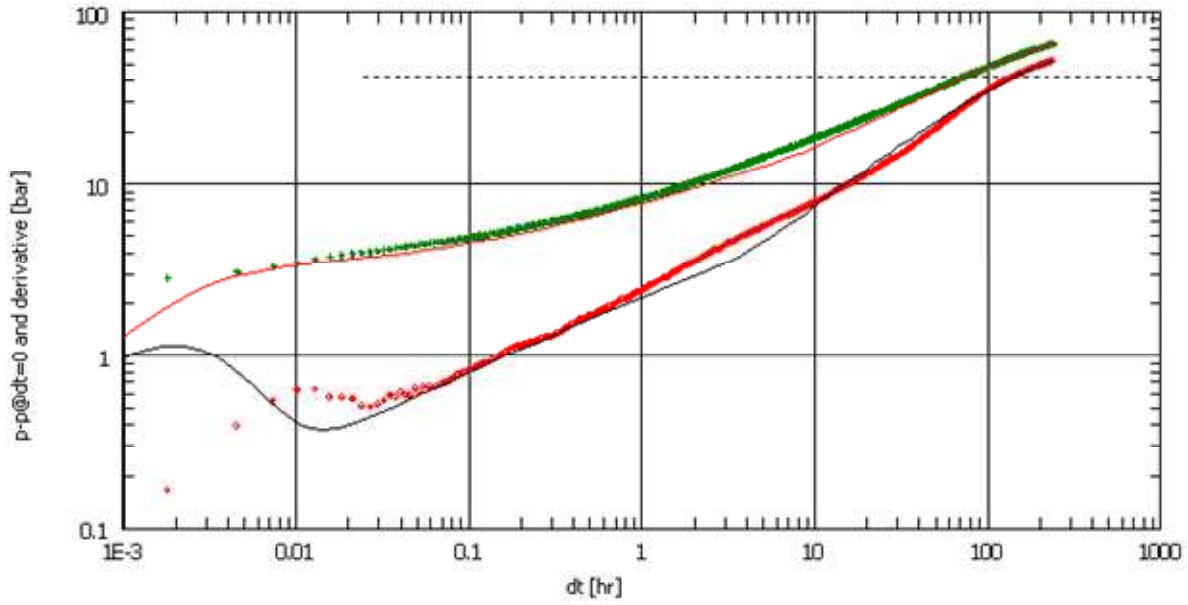


**Figure 9 – Match of the LTT FO data with a uniform-flux fracture and a nearby parallel no-flow boundary.**

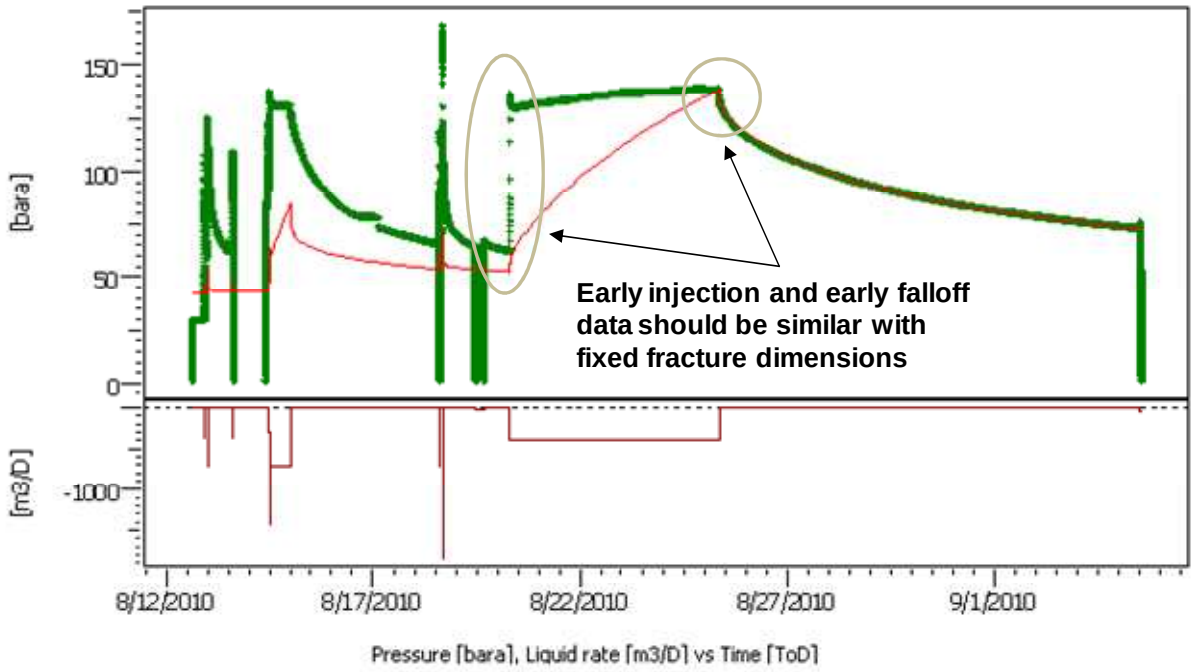


**Figure 10 – Attempted match of the entire DH4 test sequence with the LTT falloff model with a single no-flow boundary.**

The main results and key parameters of the analyses above are listed in Table 5.

| **Table 5 – Input and derived parameters from the simple analytical LTT falloff model.** | | |
|---|---|---|
| Formation thickness (assumed) | 30 | m |
| Permeability (assumed) | 1.5 | md |
| Flow capacity (assumed) | 45 | md·m |
| Fracture half-length | 420 | m |
| Fracture skin | 0.5 | |
| Storage constant | 0.01 | $m^3$/bar |
| Nearby boundary | 50 | m (parallel to fracture) |
| Model initial pressure | 42.53 | bar (at gauge) |
| Pressure at shut-in | 138.26 | bar (at gauge) |
| Rate at shut-in | 403.2 | $m^3$/d |
| Injectivity index (transient) | 4.21 | $m^3$/d/bar |
| Radius of investigation | 406 | m (at 244 hrs) |

## 3.2. Attempted Match of the Run 4 Falloff with Fracture and a No-Flow Boundary

To test out the validity of the model from Table 5 an attempt was made to match the falloff from Run 4 with the same model. The result is shown in Figure 11, where it is obvious that a single boundary at 50 m is not sufficient to match this falloff. Figure 12 shows how the match is improved if the boundary is placed only 12 m from the fracture, but even this is not enough to match late data.

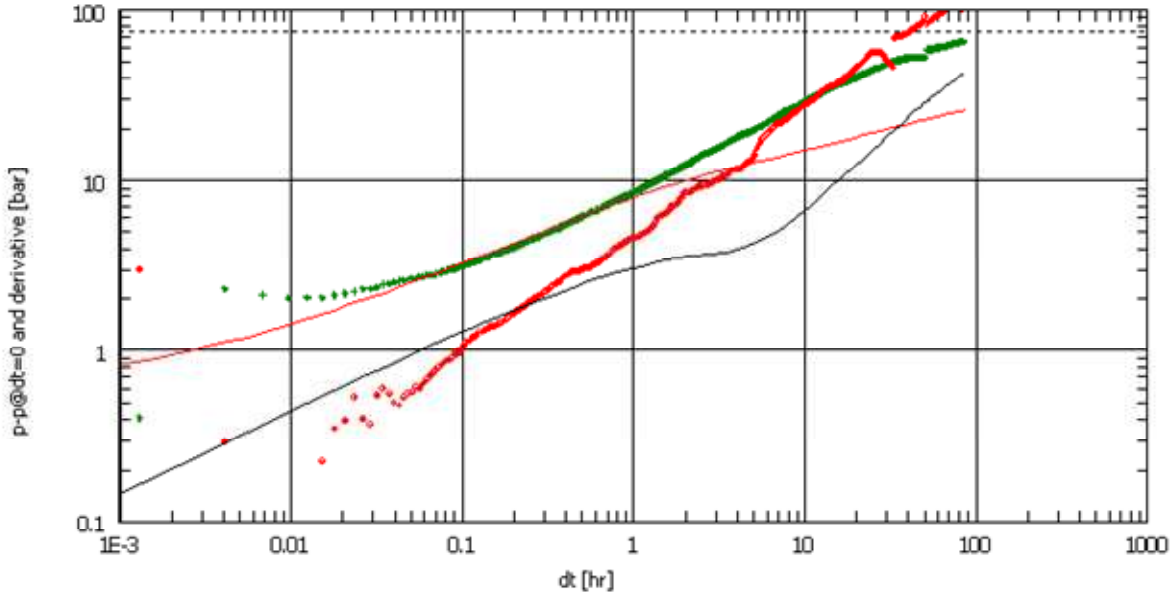


**Figure 11 – Match of the Run 4 falloff with the model from Table 5.**

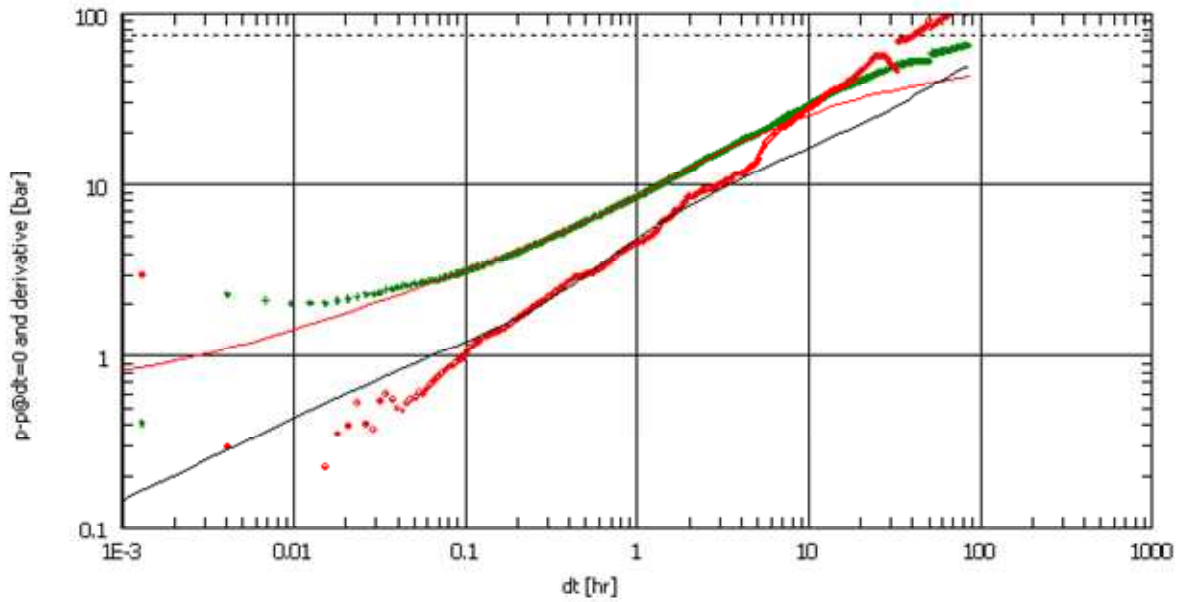


**Figure 12 – Match of the Run 4 falloff with a modified version of the model above with the boundary at 12 m.**

A logical choice to try to improve the match from Figure 12 further is to introduce one more no-flow boundary on the other side of the fracture, but parallel no-flow boundaries at distances much less than the fracture half-length does not yield pressure data anything like the falloffs from DH4, so a different approach must be taken. Another apparent failure of the model is the poor match of early falloff data in Figure 12, but this is caused by poor early data as highlighted in Figure 13.

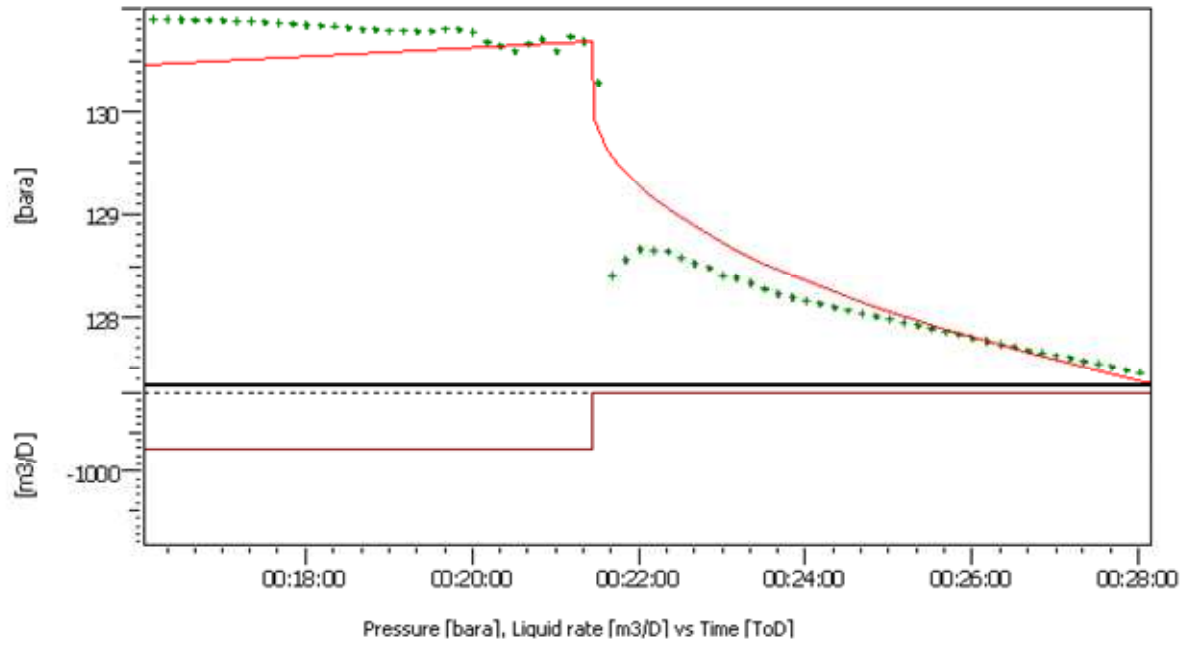


**Figure 13 – Early falloff data from Run 4 exhibiting poor data quality.**

# 4. NUMERICAL MODELS WITH FRACTURE AND MULTIPLE PARTIALLY SEALING PARALLEL BOUNDARIES

Since models with a fracture and parallel sealing boundaries failed to match the characteristics of the falloffs from Run 2, 4 and 5, a natural alternative approach is to try partially sealing boundaries. One reason is that such boundaries can produce steep falloff derivatives as seen in for instance Figure 6. However, working with several such boundaries and four data sets is challenging because the boundaries should match the pressure response of all of the falloffs in terms of location, but not necessarily in terms leakage. The point is that due to increased pressure from injection it is possible for the leakage through nearby boundaries to improve during the test sequence.

In order to include partially sealing boundaries near fractures it is necessary to use numerical models. A base case was therefore set up similar to the analytical model used above for the LTT falloff with thickness 30 m and permeability 1.5 md. Even though numerical models are more flexible, achieving excellent matches of all falloffs with a consistent model is not realistic. Since the results from the analyses also depend on the chosen thickness and permeability, there is no reason to use an excessive number of iterations in an effort to obtain excellent matches. The main objective pursued in these analyses was therefore only to prove that the test data are consistent with a reservoir model dominated by partially sealing boundaries parallel to the fracture. It is not possible, however, to quantify the spacing directly since both the fracture dimension and distances obtained from analyses depend on the assumed values of permeability and thickness, which are not known.

## 4.1. Match of the Run 4 Falloff

It was shown above that the falloff from Run 4 cannot be matched with a simple model with a fracture and a single no-flow boundary, and it was also pointed out that this falloff cannot be matched with two no-flow boundaries either. It is possible, however, to obtain a fairly good match with a numerical model having several partially sealing boundaries parallel to a long infinite-conductivity fracture. The fracture type is changed from uniform flux, as used above, to infinite conductivity since uniform flux is only chosen in analytical models for mathematical convenience.

Figure 14 shows a loglog match of the Run 4 falloff with a numerical model having an infinite-conductivity fracture with half-length 400 m and four partially sealing parallel flow barriers, two on one side at 6 and 135 m from the fracture, and two on the other side at 20 and 35 m. The area of the model and the length of the flow barriers were chosen sufficiently large such that the length of the flow barriers and the outer boundary of the model do not affect the pressure response. In the Saphir numerical model each of the barriers were given a “leakage” factor (transmissibility multiplier), with the following values chosen: 0.018 (at -6 m), 0.2 (at -135 m), 0.02 (at 20 m) and 0.001 (at 35 m), with negative distances on one side of the fracture and positive distances on the other. Note also that Leakage = 0.001 is low but not fully sealing (0).

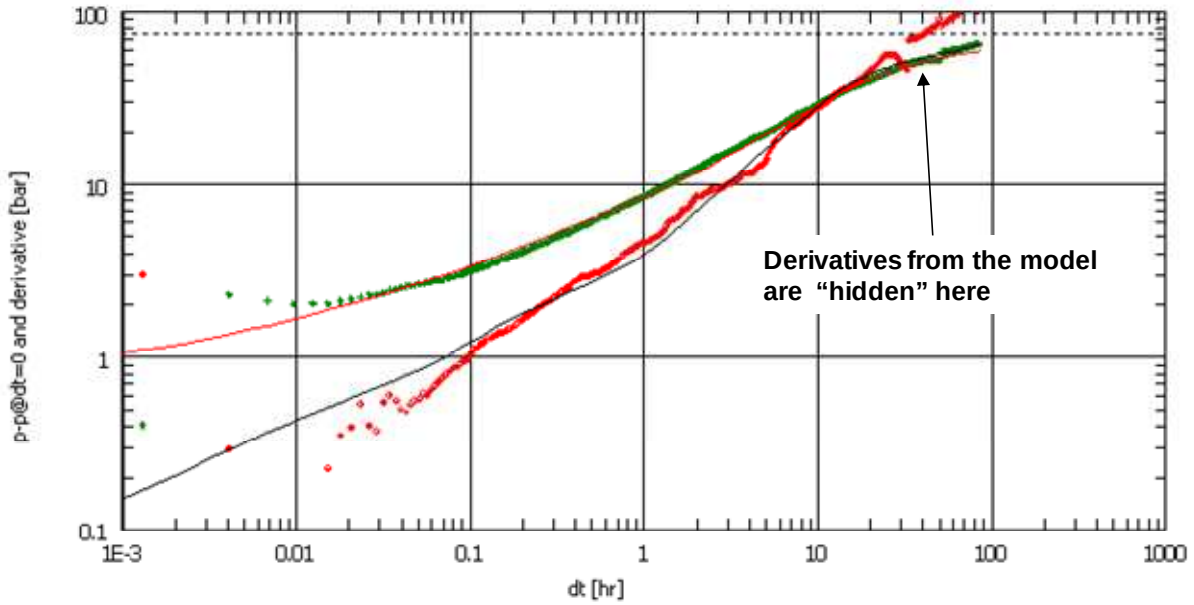


**Figure 14 – Match of the Run 4 falloff with a numerical model with a fracture and partially sealing boundaries.**

A match of the numerical model above with the entire data set is shown in Figure 15 with a detail of the same match shown in Figure 16. For this test the pressures recorded at the wellhead reached a local minimum 20.8 hrs after shut-in, increased to a local maximum around 30 hrs after shut-in and again started falling towards atmospheric pressure at around 68 hrs after shut-in. These times correspond to total elapsed times of 78.1, 87 and 125 hrs on the time scale used in Figure 16, and hence do not correspond to the local gradual increase and drop in down-hole pressure observed between 98 and 108 hrs on the same time scale. The cause for the pressure disturbance in the down-hole data is not clear.

Note that the linear pressure trend observed in the down-hole pressures after the disturbance is not matched by the numerical model. Nor does the initial pressure of the model match the initial pressure recorded in the well. In order for the initial pressure of the model to approach the value 29.6 bar from the well, it will probably be necessary to add more flow barriers. This approach was tried, but it is a very slow and time-consuming process, with the results above eventually considered satisfactory as a means to get a realistic model of formation heterogeneities. The point is that all four falloffs have to be considered if a change is going to be considered an improvement.

Considering the meaning of the initial pressure from the model, this is the value where the computation must start to match the flowing pressure at the time of shut-in for the falloff being modelled. Even if the model had produced an excellent match of the entire falloff, it is not clear to what extent it could have been used as a reliable estimate of the initial pressure. Using Horner extrapolation of the falloff data to get an estimate of the initial pressure is also unreliable for data with severe boundary effects. The problem is that Horner extrapolation assumes the data to be dominated by radial flow.

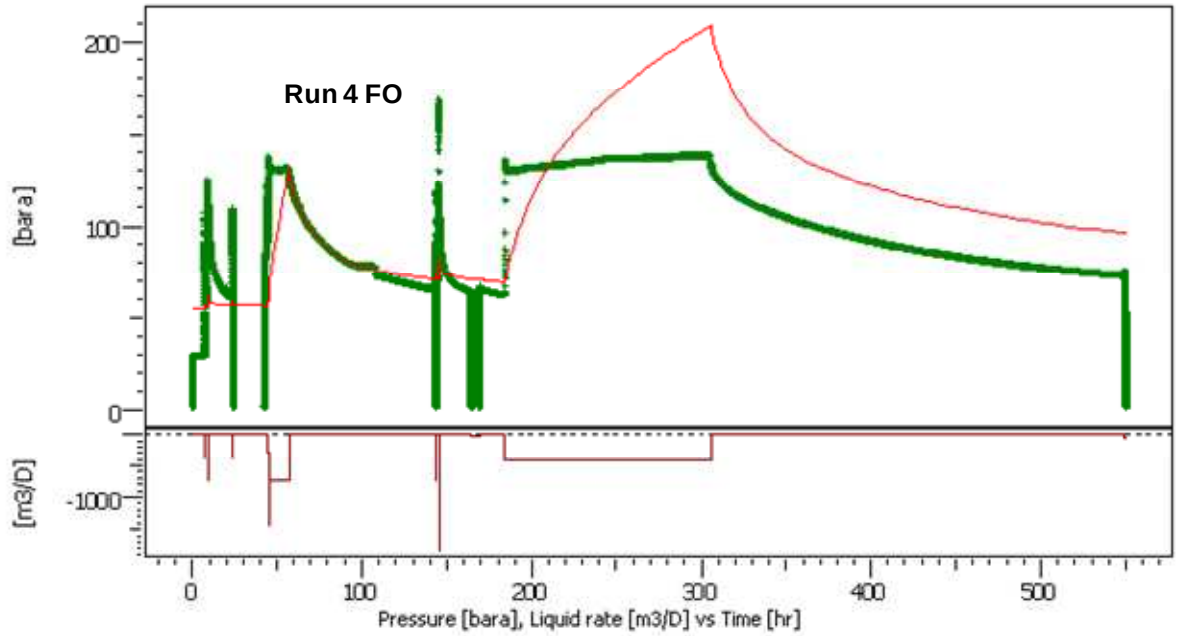


**Figure 15 – Match of the entire DH4 data set with the Run 4 falloff model.**

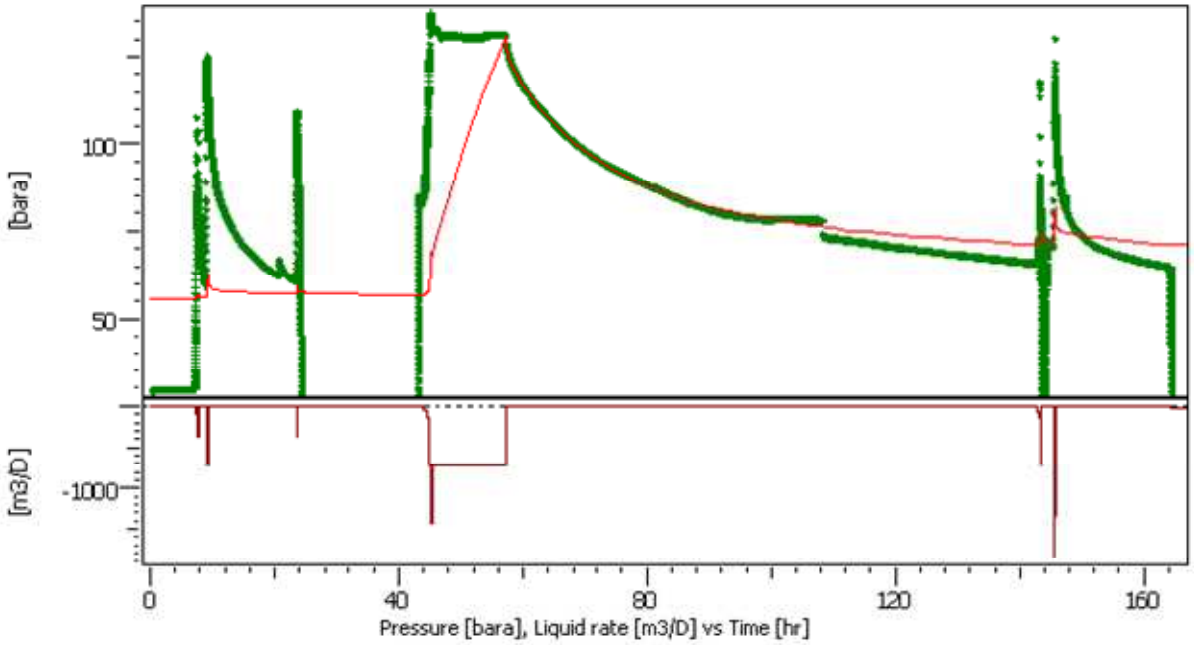


**Figure 16 – Detail of the match from Figure 15 with emphasis on the Run 4 period.**

## 4.2. Match of the Run 2 Falloff

An attempt was made to match the falloff from Run 2 with adjusted fracture half-length and modified leakage parameters through the boundaries, but this approach did not lead to an acceptable match. The approach that was used instead was to reduce the fracture half-length to 54 m and add two new boundaries. Figure 17 shows how this modified model matches the Run 2 falloff. The timing is off, but the major features in the data are reproduced by the numerical model. Since matching a minifrac falloff is often quite difficult, the match of the Run 2 falloff has to be considered acceptable. The new boundaries, which have been located at distances of only 2 and 5 m from the fracture, are not needed for the other falloffs, possibly as a result of communication through these being established during the 12 hrs injection period from Run 4.

Even though an acceptable match of late data was not achieved without these new boundaries, it does not necessarily imply that two new boundaries are needed. One might be enough, and with a lucky combination of leakage parameters it might even be possible to get an acceptable match based on the Run 4 model. The challenge is the number of iterations and time required to do these analyses.

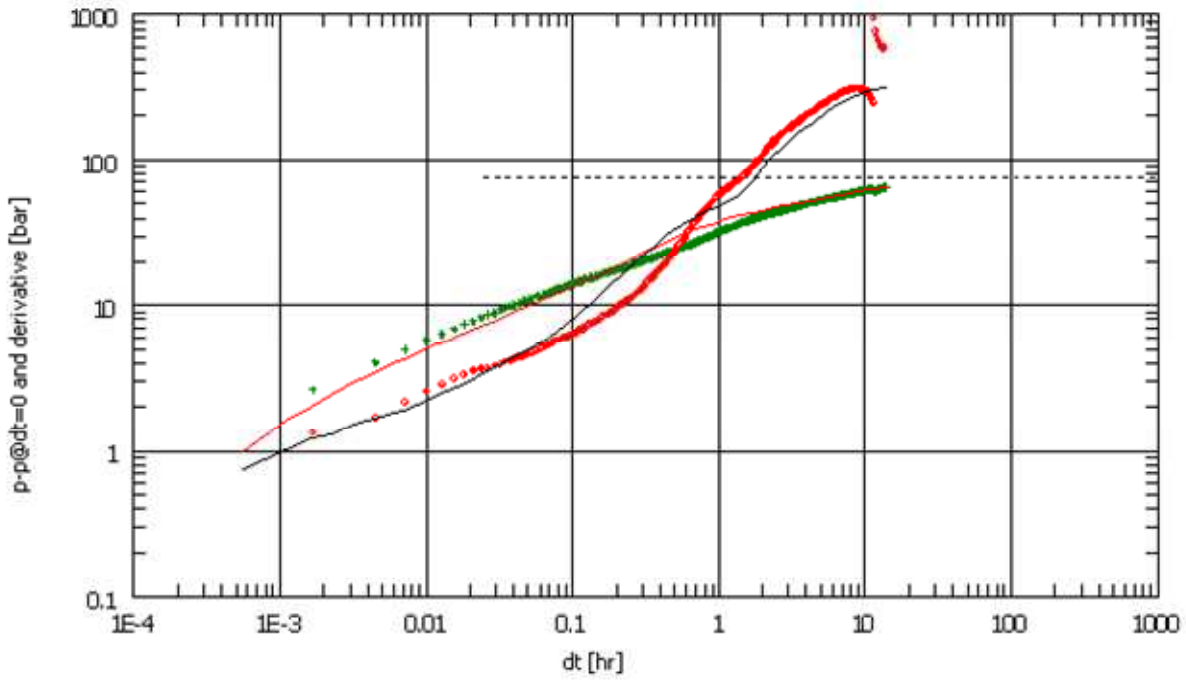


**Figure 17 – Match of the Run 2 falloff with a modified numerical model with a fracture and partially sealing boundaries.**

Figures 18 and 19 show how the Run 2 model matches the overall and early part of the pressure response from DH4. The pressure is seen to drop too fast early in the falloff and perhaps too slowly towards the end. It is also clear that the model initial pressure does not come close to the initial pressure recorded in the well. In an attempt to match the recorded

initial pressure the natural approach would be to add boundaries or adjust the leakage through the existing boundaries, or both. Again, this is very time consuming, and was therefore stopped with the choices shown above.

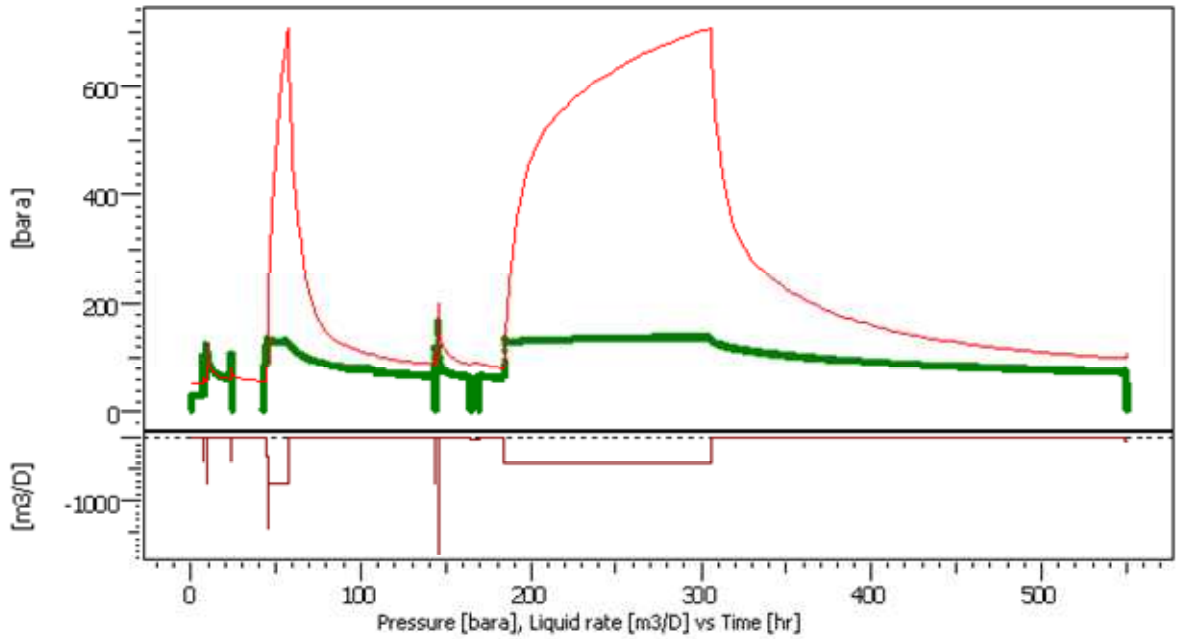


**Figure 18 – Match of the entire DH4 data set with the Run 2 falloff model.**

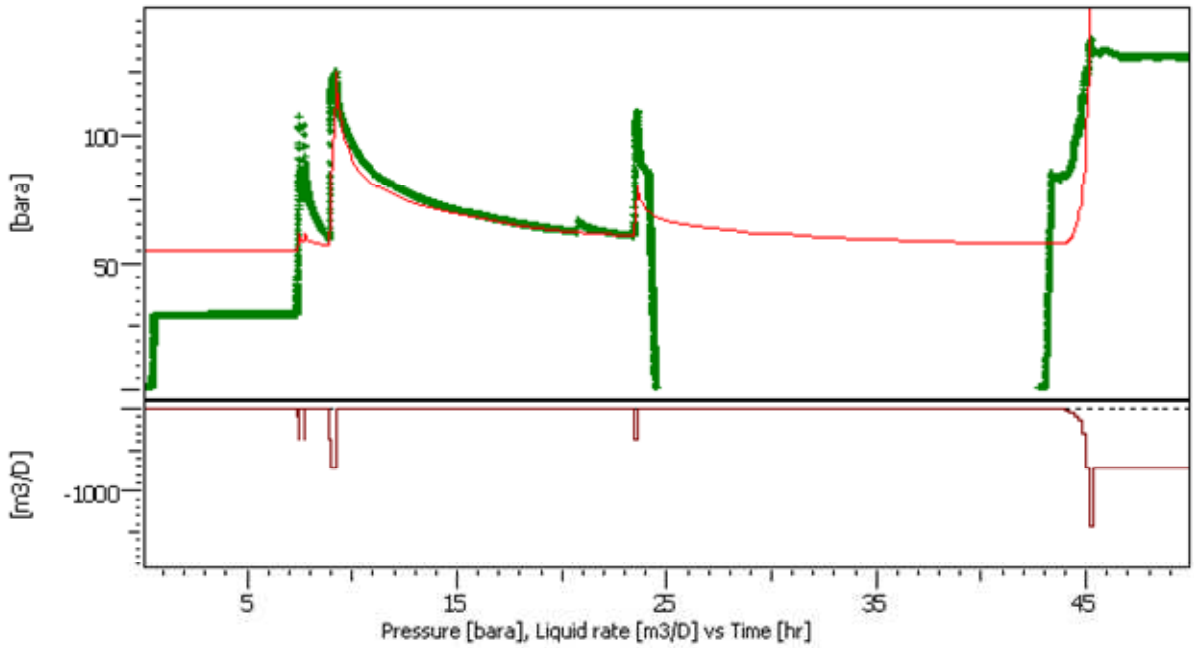


**Figure 19 – Detail of the match from Figure 18 with emphasis on the Run 2 data set.**

Note that the pump pressure went from positive to vacuum roughly 1.7 hrs into the falloff, but this did not affect the down-hole pressures significantly, although a slight change in derivative trend is perhaps detectable in the loglog plot. Another event 11.6 hrs into the falloff is clearly visible in the data. This corresponds to the pump being opened to atmospheric pressure.

Key boundary parameters from the four analyses are listed in Table 6 below, and key model parameters in Table 7. Table 7 also includes the radius of investigation at the end of each falloff. This is the distance into the formation with pressure response affecting the wellbore pressure.

## 4.3. Match of the Run 5 Falloff

It turns out to be easier to match the falloff from Run 5 with a modified version of the model used for Run 4 compared to the same effort for Run 2. Run 5 is also a minifrac test, just like Run 2, with a short flow and short falloff. The injection rate for Run 5 was, however, much higher.

The chosen match of the Run 5 falloff with a fracture half-length of 65 m is shown in Figure 20. This match is quite good, even though there are some timing issues with the match.

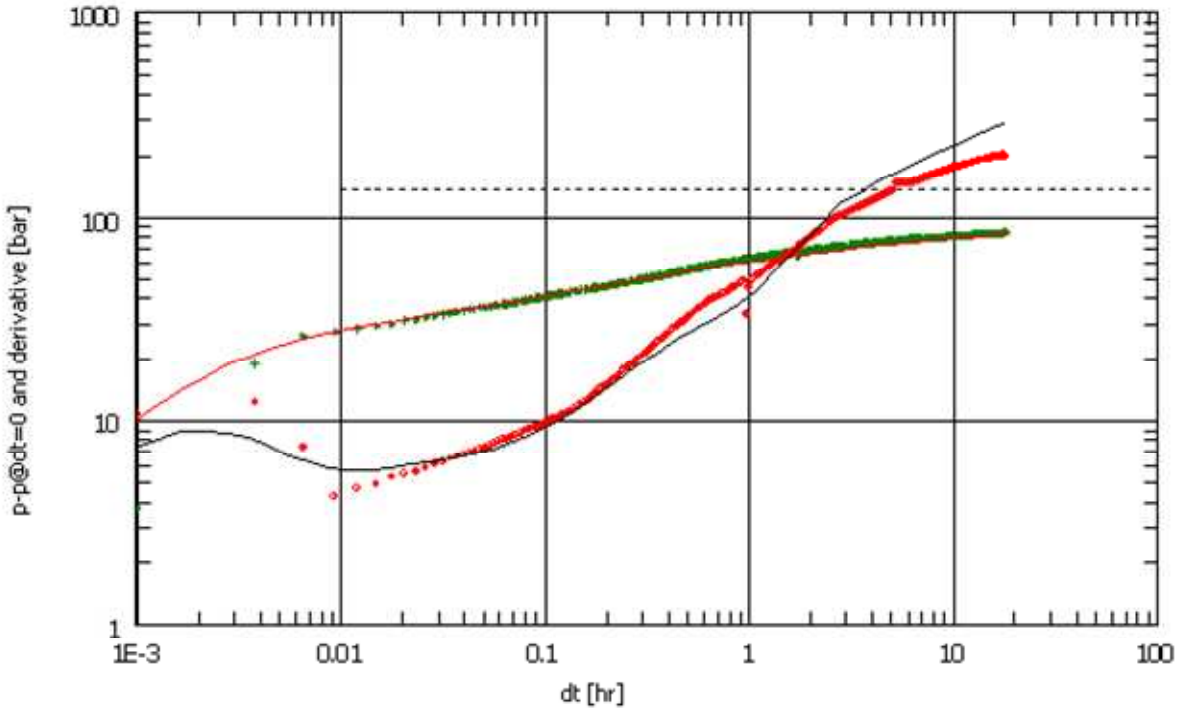


**Figure 20 – Match of the Run 5 falloff with a numerical model with a fracture and partially sealing boundaries.**

Figure 21 shows how the Run 5 model matches the entire data set from DH4, and Figure 22 how the model matches the data segment from Run 5. The match is not perfect but still quite good. The match of the initial pressure is difficult to make out in Figure 21, but the model initial pressure for the Run 5 falloff is 28.9 bar, which is just below the value 29.6 bar recorded in the well.

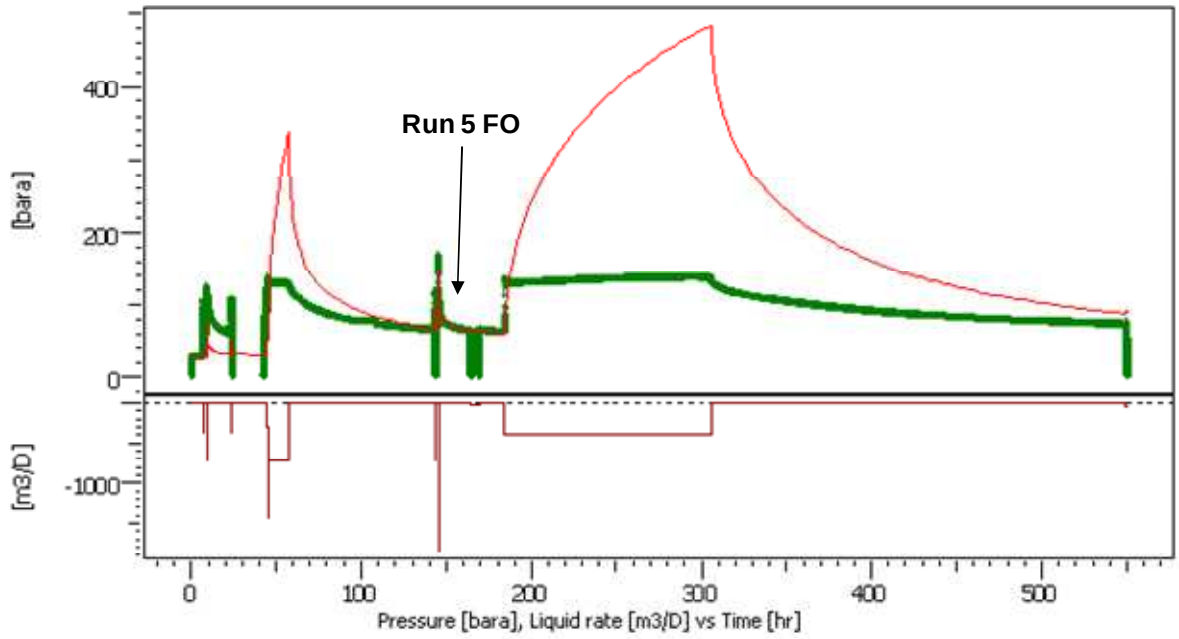


**Figure 21 – Match of the entire DH4 data set with the Run 5 falloff model.**

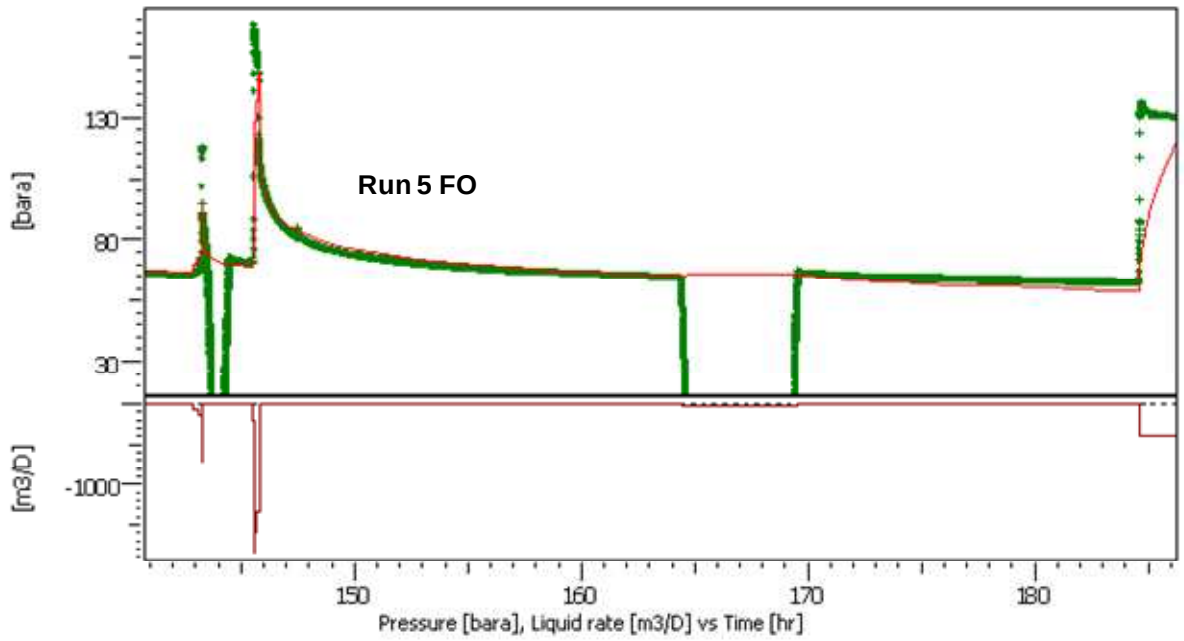

**Figure 22 – Detail of the match from Figure 21 with emphasis on the Run 5 data set.**

Without any additional information about the formation pressure it would be difficult to choose between values obtained from the first three runs. This is a real problem for these data sets with considerable boundary effects caused by partially boundaries with changing leakage and in addition a dynamic fracture model. Since the gauge has been rerun in the well for long-time measurements, new and more accurate estimates will be possible later.

## 4.4. Match of the LTT Falloff

A modified version of the numerical model can also be used to match the falloff from the long-time test with a fracture half-length of 400 m. This is shown in Figure 23, which is similar to the match in Figure 9 above, but better.

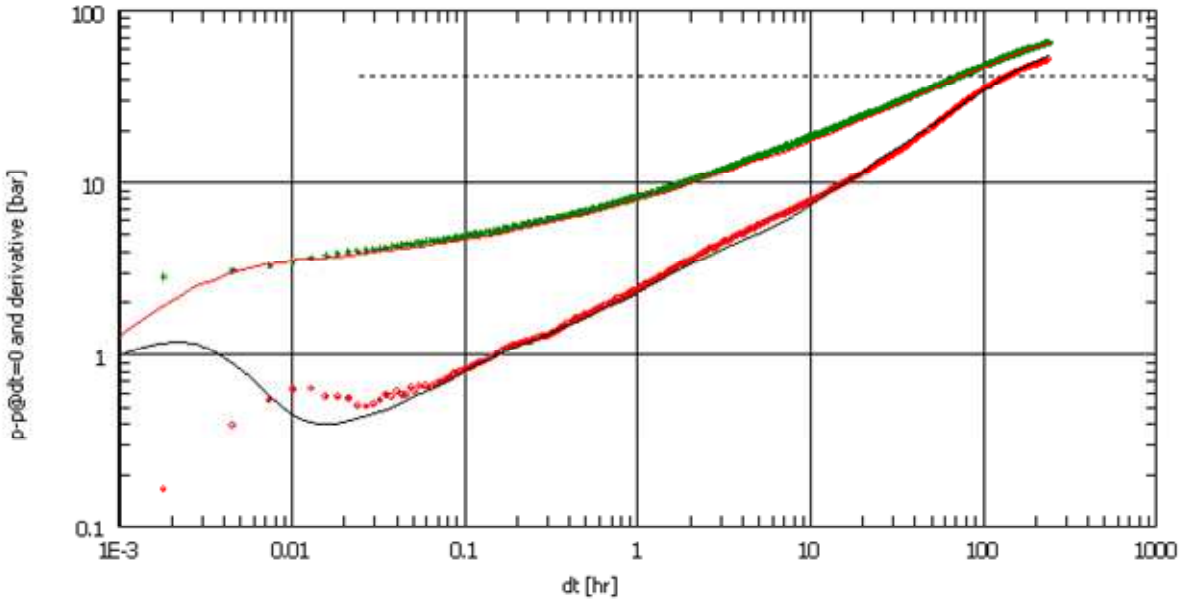


**Figure 23 – Match of the LTT falloff with a numerical model with a fracture and partially sealing boundaries.**

A match the entire test sequence from DH4 with the LTT falloff model is shown in Figure 24. The match of the falloff is excellent, but it does not match the injection period from the LTT, nor the earlier test runs. The initial pressure from the model, at 45.48 bar, is also too high compared to the measured initial pressure in the well.

It would be possible to subdivide the injection period into many parts and use a model with fracture half-length specified for each period. One could then get a direct picture of how the fracture needs to grow to match the down-hole pressures. This is a time-consuming effort, and was therefore not pursued, especially since it cannot handle changing leakage factors, and hence not the complete dynamic picture.

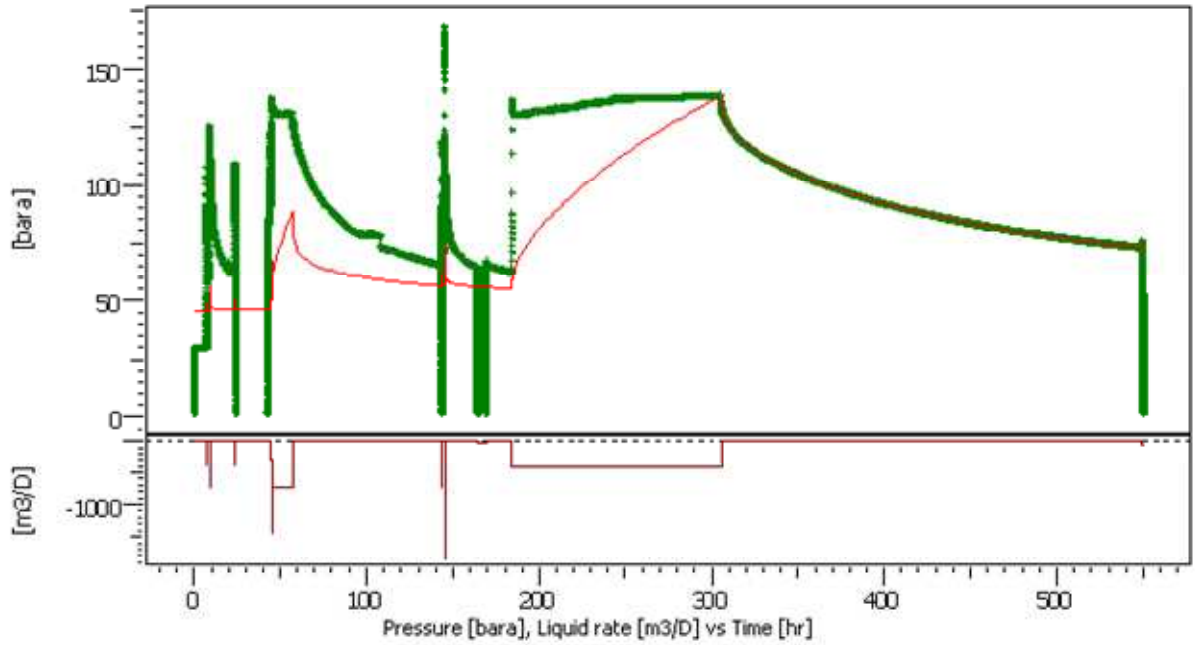


**Figure 24 – Match of the entire DH4 data set with the LTT falloff model.**

## 4.5. Summary of Results from the Numerical Models

Table 6 lists the key parameters of the partially sealing boundaries. As was pointed out above, the length of the boundaries and the area of the model were chosen to be large enough such that the numerical models will behave as infinite for the periods modelled. Considering the boundaries listed in Table 6, those at -2 and 5 m were only used for Run 2. The boundary at -135 m was also only included for Run 4 and the LTT, since it is too far from the fracture to affect the data from Runs 2 and 5.

Note also that the leakage of the boundary at -6 m has been reduced slightly from Run 2 to Run 4, while the others either stay constant or improve with time. This “opposite” behaviour of the boundary at -6 m is assumed to be caused by the added boundary between it and the fracture as a minor grid effect in the numerical model.

**Table 6 – Partially sealing boundaries.**

| Location (m) | Leakage (transmissibility multiplier) * | | | |
|---|---|---|---|---|
| | Run 2 | Run 4 | Run 5 | LTT |
| 35 | 0.001 | 0.001 | 0.001 | 0.008 |
| 20 | 0.018 | 0.02 | 0.04 | 0.06 |
| 5 | 0.001 | - | - | - |
| -2 | 0.018 | - | - | - |
| -6 | 0.02 | 0.018 | 0.02 | 0.2 |
| -135 | - | 0.2 | - | 0.2 |

*) No value listed implies corresponding boundary was not used.

Other key results from the numerical models are listed in Table 7, while basic properties such as thickness and permeability are the same as in Table 5, with thickness 30 m and permeability 1.5 md.

| Table 7 – Individual results from the falloff analyses. | | | | |
|---|---|---|---|---|
| | **xf (m)** | **Sf** | **pi (bar)** | **rinv (m)** |
| **Run 2** | 54 | 0.0116 | 54.80 | 98 |
| **Run 4** | 400 | 0.07 | 55.74 | 240 |
| **Run 5** | 65 | 0.165 | 28.91 | 112 |
| **LTT** | 400 | 0.5 | 45.48 | 406 |

## 5. PARAMETER DEPENDENCE OF RADIAL- AND LINEAR-FLOW DATA

The pressure change for radial-flow data under constant rate injection is given in the form

$$\Delta p = m \cdot \log t + b \qquad (1)$$

with b denoting a constant which depends both on model parameters and skin (damage or stimulation) and m is the semilog slope given by the identity

$$m = \frac{21.49 q B \mu}{kh} \qquad (2)$$

in terms of practical SI units (bar, md and metric). Since the derivatives included in loglog plots are based on the natural logarithm, the derivative value corresponding to radial flow will be given by

$$\frac{d\Delta p}{d\ln t} = m \frac{d\log t}{d\ln t} = \frac{m}{\ln 10} \ . \qquad (3)$$

It follows that radial flow data will have a constant derivative value, given by Eq. 3, and hence will be easy to spot on a loglog plot. Note also that if the well is located close to a no-flow boundary, then late data will correspond to flow from a half-circle. Such data, with flow from one side are referred to as hemi-radial. These will exhibit a constant derivative with twice the value from Eq. 3.

For falloff data following a period with constant or variable injection, the simple elapsed time t above is replaced by a modified time expression and the rate q with the last stable value prior to shut-in. The modified expressions are automatically chosen by the software, with the key identities used in analyses for practical purposes being the same.

For fractured wells one expects a portion of early data to be dominated by or at least heavily influenced by transient linear flow. For simple constant rate injection the pressure change in the well should then take the form

$$\Delta p = m'\sqrt{t} + b \qquad (4)$$

with b denoting a constant accounting for effects of flow restrictions ("damage") in or near either the well or the fracture, and

$$m' = \frac{0.6236qB}{hx_f}\sqrt{\frac{\mu}{k\varphi c_t}} \qquad (5)$$

is the slope of the pressure data plotted vs $\sqrt{t}$ . Note also that the derivative of Eq. 4 is given by

$$\frac{d\Delta p}{d\ln t} = m'\frac{d\sqrt{t}}{d\ln t} = \frac{m'}{2}\sqrt{t} \quad . \qquad (6)$$

For falloff data following a period with constant or variable injection, the simple elapsed time t above is replaced by a modified time expression and the rate q with the last stable value prior to shut-in. The modified expressions are automatically chosen by the software, with the key identities used in analyses therefore for practical purposes being the same. Our challenge is therefore basically the same, even with q, B, μ, and perhaps h, known from direct measurements, we cannot determine $x_f$ unless k, φ and $c_t$ are known. This situation is different from radial-flow data, where the slope of the pressure data plotted vs logt only depends on the product kh in addition to q, B and μ. For non-fractured wells we also have better control of the thickness h compared to fractured wells where non-detected vertical fracture growth might be possible.

For short fractures and long shut-in periods it is possible that radial-flow behavior will be reached or at least indicated at the end of a falloff, and thus allow a reasonable estimate of k to be obtained, but there can still be uncertainty in the effective porosity and total system compressibility, and hence in the estimated fracture half-length. For the analyses in this report the porosity and total compressibility have been kept constant as listed in Table 4. From Eq. 5 it follows that if the product of φ and $c_t$ is increased, then a similar reduction must be applied to k.

Figure 25 illustrates the ideas above, with the half-slope line corresponding to Eq. 6 and the two horizontal dashed lines based on either Eq. 2 for simple radial flow, or double that value for hemi-radial flow. These lines correspond to the simple analysis shown in Figure 9 with results listed in Table 5.

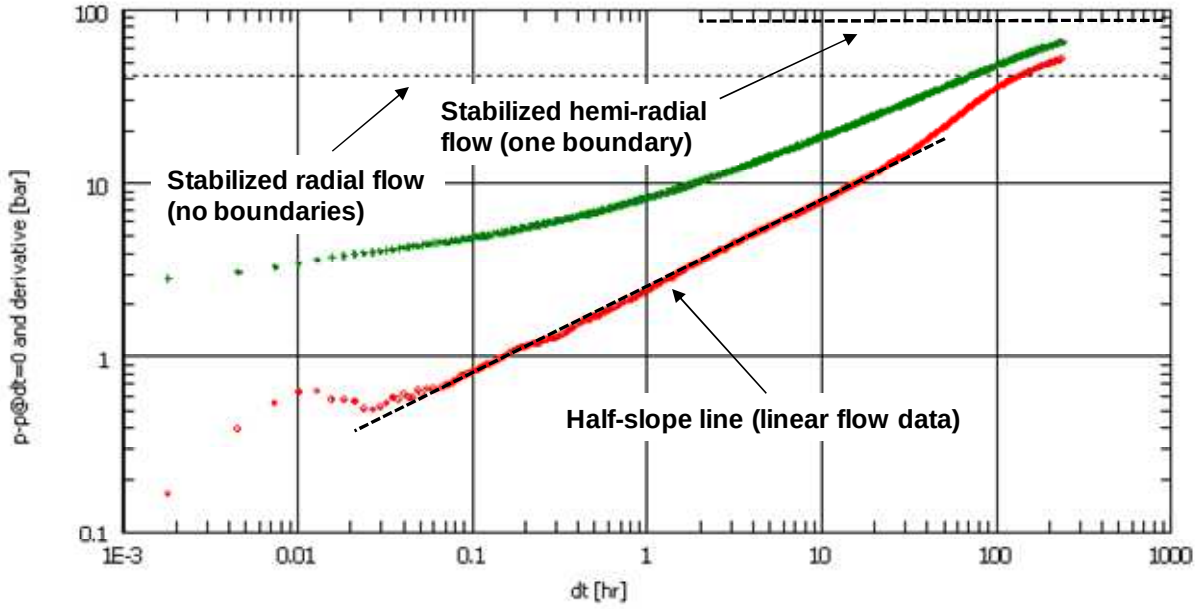


**Figure 25 – Key flow regimes present or possible in the LTT falloff data.**

## 6. ANALYSES WITH THE SAME FLOW CAPACITY BUT A CHANGE IN THICKNESS

If radial flow data have been identified from test data, then the flow capacity, or kh product, will be known, but there could be uncertainty concerning the thickness. For such cases it follows from the results above that if the thickness is changed by the factor F, then the permeability must be changed by the factor 1/F, and vice versa. Moreover, if the permeability is changed by the factor F, then distances and lengths must be changed by the factor $\sqrt{F}$. The latter point was not discussed above, but will be illustrated with the DH4 data.

For fractures the situation is similar and determined by Eq. 5. The point is, if k and h are changed but the kh product kept constant, then in order for the slope to remain unchanged the fracture half-length must change as $\sqrt{k}$. The point is that the ratio $x_f/\sqrt{k}$ must remain unchanged. This observation is consistent with the claim above that a change in permeability by a factor of F requires the fracture half-length, and other lengths, to be changed by a factor of $\sqrt{F}$. For numerical models with partially sealing boundaries the leakage multipliers need not be changed since these are relative quantities.

### 6.1. A Modified Base Case with Thickness 90 m and Unchanged kh Product

The base case has a thickness of 30 m and a kh product of 45 md·m. With thickness increased to 90 m the permeability must be reduced to 0.5 md. Lengths and distances must therefore be changed with the factor $1/\sqrt{3}$. Based on values listed in Table 5, the modified

model will have a half-length of $420/\sqrt{3} = 242.5$ m and a distance of $50/\sqrt{3} = 28.9$ m to the no-flow boundary.

A loglog match of the LTT falloff with the modified model is shown in Figure 26 with fracture skin 0.097. The match is identical to that shown in Figure 9, with additional plots not necessary.

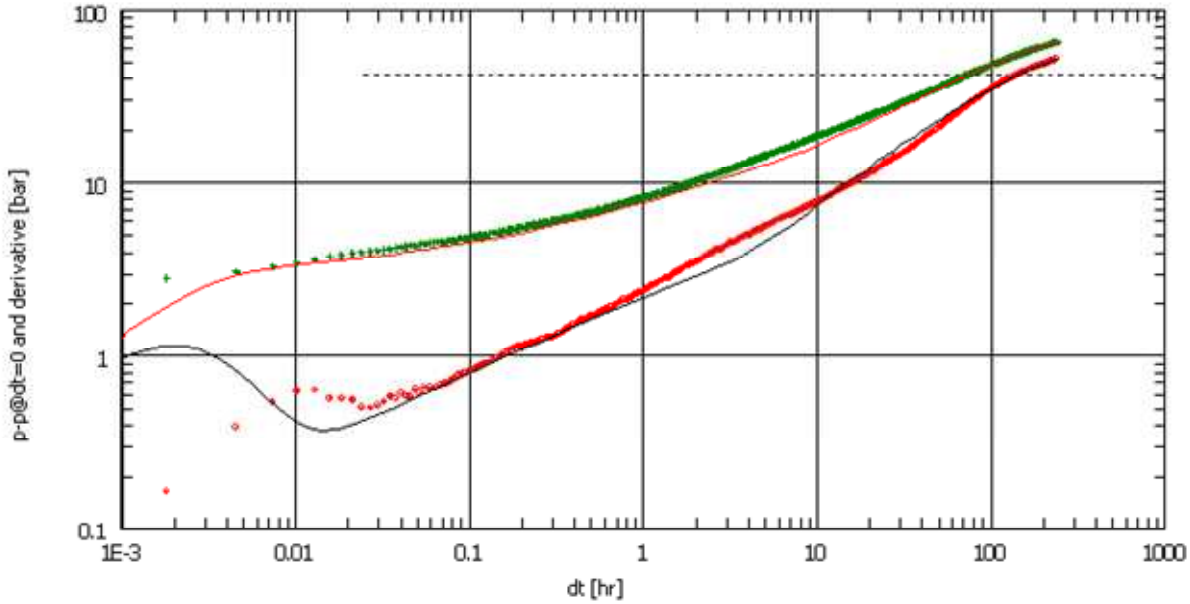


**Figure 26 – Match of the LTT falloff with a modified version of the model from Table 5 with thickness 90 m and permeability 0.5 md.**

## 7. ANALYSES WITH THE SAME PERMEABILITY BUT DIFFERENT THICKNESS

This case is different from the one above with unchanged flow capacity since a change in thickness without a change in permeability implies a change in flow capacity. For half-slope data it is possible to keep the slope by changing the fracture half-length such that the product $hx_f$ remains unchanged. For late data, on the other hand, in order to keep the derivative level unchanged with a change in flow capacity it is necessary to change the model. Options can be to introduce more boundary effects, if possible, or to change the permeability away from the fracture. This basically requires a new analysis to be carried out with a new reservoir model

.

### 7.1. A Modified Base Case with Thickness 100 m and Unchanged Permeability

To illustrate problems that can be involved when the thickness is changed and not the permeability, consider again a change of the base-case model from Table 5, this time with thickness increased from 30 to 100 m without changing the permeability. We then get a new

flow capacity of 150 md·m, and hence a new derivative value equal to 0.3 times the original value. However, the slope of the early linear-flow data can be maintained by reducing the half-length by the factor 0.3 from 420 to 126 m.

Figure 27 shows a match of the LTT falloff with a uniform-flux fracture with skin 0.15, half-length 126 m, increased flow capacity to 150 md·m and only a single no-flow boundary at the original distance 50 m. With the increased flow capacity a match of late data is not achieved. In order to also match late data without changing the permeability away from the well it is necessary to use at least two boundaries. The boundaries can either intersect or be parallel.

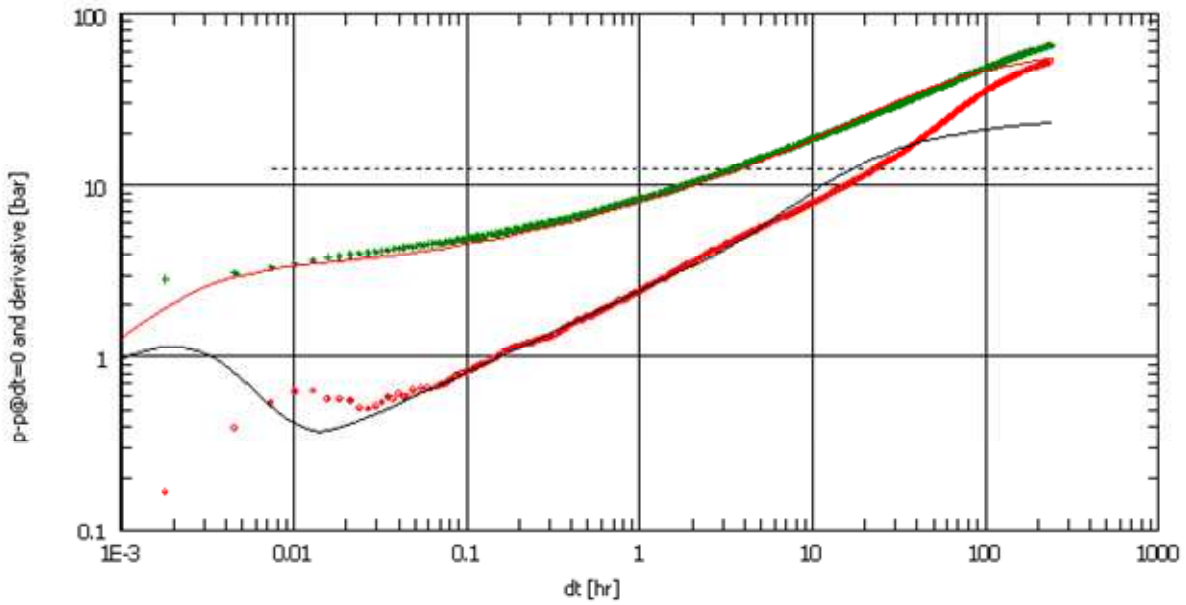


**Figure 27 – Match of the LTT FO with a modified version of the model from Table 5 with thickness 100 m and permeability 1.5 md.**

Figure 28 shows a match of the LTT falloff based on the model above with fracture half-length 126 m, flow capacity 150 md·m and parallel boundaries at 30 and 75 m. The fracture skin value in the model is till 0.15.

Although the quality of the match in Figure 28 might be acceptable, the model is too restricted with initial pressure from the model 21.18 bar. A model with boundaries intersecting at 45 degrees can also be used to match the falloff. The latter model is more open with a more realistic initial pressure of 39 bar, but neither of these models can be used for the earlier tests, and hence are not valid alternatives to the analyses above with the numerical models.

If a net thickness of 100 m with an average permeability of 1.5 md is realistic, then a new set of analyses with a numerical model with partially sealing boundaries must be run. This was tried, and can be done, but results have not been included in this report.

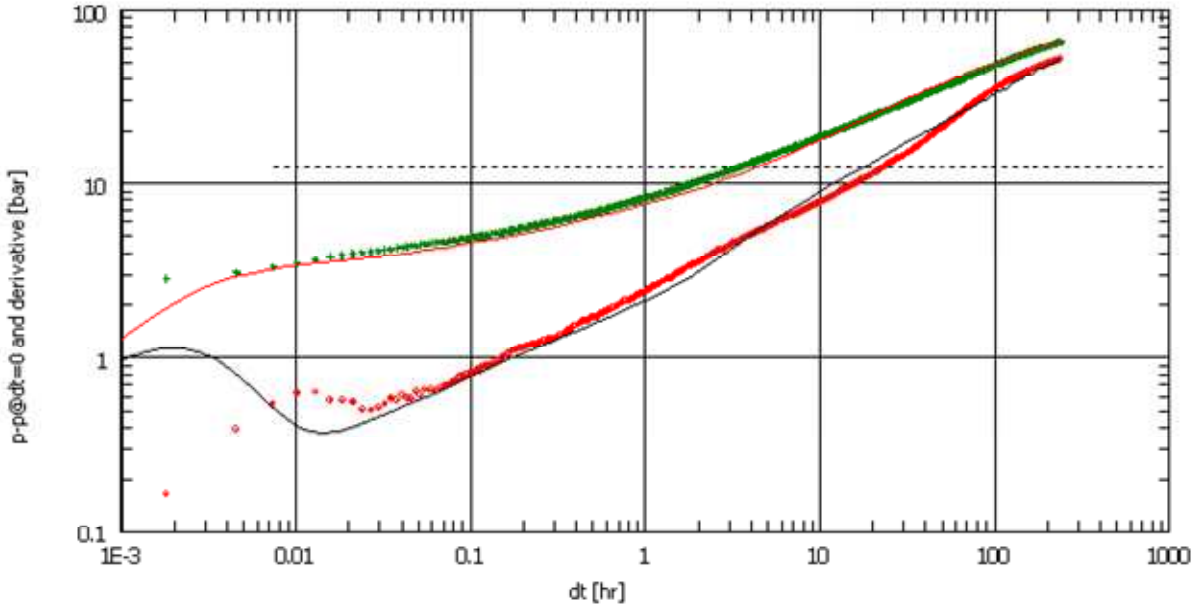


**Figure 28 – Match of the LTT FO with a modified version of the model above with parallel no-flow boundaries at 30 and 75 m.**